TISSUE-SPECIFIC PROGENITOR AND STEM CELLS

Peripheral Blood-Derived Mesenchymal Stem Cells: Candidate Cells Responsible for Healing Critical-Sized Calvarial Bone Defects

SHAOWEI LI,[a,*] KE-JUNG HUANG,[a,*] JEN-CHIEH WU,[a,*] MICHAEL S. HU,[a,*] MRINMOY SANYAL,[b] MIN HU,[a] MICHAEL T. LONGAKER,[a] H. PETER LORENZ[a]

[a]Division of Plastic and Reconstructive Surgery, Department of Surgery, and [b]Department of Pathology and Medicine, Stanford University School of Medicine, Stanford, California, USA

*Contributed equally.

Correspondence: H. Peter Lorenz, M.D., Division of Plastic and Reconstructive Surgery, Department of Surgery, Stanford University, 257 Campus Drive West, Stanford, California 94305, USA. Telephone: 650-736-1703; E-Mail: plorenz@stanford.edu

ABSTRACT

Postnatal tissue-specific stem/progenitor cells hold great promise to enhance repair of damaged tissues. Many of these cells are retrieved from bone marrow or adipose tissue via invasive procedures. Peripheral blood is an ideal alternative source for the stem/progenitor cells because of its ease of retrieval. We present a coculture system that routinely produces a group of cells from adult peripheral blood. Treatment with these cells enhanced healing of critical-size bone defects in the mouse calvarium, a proof of principle that peripheral blood-derived cells can be used to heal bone defects. From these cells, we isolated a subset of CD45⁻ cells with a fibroblastic morphology. The CD45⁻ cells were responsible for most of the differentiation-induced calcification activity and were most likely responsible for the enhanced healing process. These CD45⁻ fibroblastic cells are plastic-adherent and exhibit a surface marker profile negative for CD34, CD19, CD11b, lineage, and c-kit and positive for stem cell antigen 1, CD73, CD44, CD90.1, CD29, CD105, CD106, and CD140α. Furthermore, these cells exhibited osteogenesis, chondrogenesis, and adipogenesis capabilities. The CD45⁻ fibroblastic cells are the first peripheral blood-derived cells that fulfill the criteria of mesenchymal stem cells as defined by the International Society for Cellular Therapy. We have named these cells "blood-derived mesenchymal stem cells." STEM CELLS TRANSLATIONAL MEDICINE 2015;4:1–10

INTRODUCTION

A key theme in regenerative medicine is repair of damaged tissue with treatment using stem/progenitor cells. For example, bone defects can be treated with stem/progenitor cells isolated from bone marrow [1] and adipose tissue [2]. However, the processes of isolating these stem/progenitor cells, such as bone marrow aspiration and liposuction, are invasive. Cells that have similar regenerative function and can be isolated with minimal or no invasive procedure will greatly simplify the bone healing process. Peripheral blood is an ideal alternative source for these cells owing to the ease of cell retrieval and blood bank storage. Peripheral blood is also known to host many stem/progenitor cells, such as peripheral blood stem cells, which are used in bone marrow transplantation therapy [3], and endothelial progenitor cells, which have long been recognized to participate in new blood vessel formation [4]. A frequently discussed cell is the mesenchymal stem cell (MSC), which is a multipotent stromal cell with prominent regenerative functions. The MSC is an ideal candidate for many cell-based therapies, including enhanced healing of bone defects [1, 5, 6]. MSCs have been isolated from

various tissues [7, 8], including bone marrow, fat, and muscle. However, the existence of MSCs in the peripheral blood has not been confirmed (as described in the Discussion) [9–11].

Cells cultured from peripheral blood have been hypothesized to be able to enhance bone healing. For example, fibrocytes [12] and monocyte-derived mesenchymal progenitor cells [13] are capable of in vitro calcification in response to differentiation signals. Moreover, circulating skeletal stem cells [14] and circulating osteoblasts [15] are capable of bone formation when placed in subcutaneous pockets of animals. Only one study has shown circulating cells to have enhancement of bone healing in vivo. In that study, an undefined MSC-like population was shown to improve healing in the rabbit ulna [16]. However, the identity of the MSC-like cells was not clear (discussed further in the Discussion).

In the present study, we define a population of cells derived from the peripheral blood that can heal critical-sized bone defects. Unlike previous studies investigating cell-based therapy to enhance long bone healing through endochondral ossification [16], we investigated and defined a cell population that can enhance healing of calvarial bone defects through intramembranous

ossification. In isolating the cells responsible for the healing process, we discovered a population of nonhematopoietic cells that fulfill the MSC criteria, as defined by the International Society for Cellular Therapy (ISCT). We have named these cells "blood-derived mesenchymal stem cells" (BD-MSCs).

MATERIALS AND METHODS

Peripheral Blood Collection and Heavy Fraction Cellular Isolation

All experiments were performed in accordance with the Stanford University Animal Care and Use Committee guidelines (protocol identification [ID] no. 11048). The peripheral blood was collected from male FVB-L2G, FVB-luciferase (Luc)-green fluorescent protein (GFP), or FVB mice (Jackson Laboratory, Sacramento, CA, http://www/jax.org) or CD-1 mice (Charles River Laboratories International, Inc., Wilmington, MA, http://www.criver.com) at the age of 7 to 8 weeks, depending on the experimental design. Among them, only cells from FVB-L2G mice exhibit strong green fluorescence that can be detected with fluorescence microscopy. To collect peripheral blood, the mice were anesthetized with isoflurane (Butler Schein Animal Health, Encinitas, CA, https://www.henryscheinvet.com) and injected with 4 U of heparin (Sigma-Aldrich, St. Louis, MO, http://www.sigmaaldrich.com) through retro-orbital veins. After 5 minutes, the mice were bled from the retro-orbital vein, and the blood was collected into a 1.5-ml microcentrifuge tube containing 1 U of heparin in 100 μl of phosphate-buffered saline (PBS; Life Technologies, Carlsbad, CA, http://www.lifetechnologies.com). The blood collected from each mouse was 1 to 1.3 ml routinely. To lyse red blood cells, 3 ml of blood was mixed with 30 ml of red blood cell lysis buffer (NH_4Cl 8.3 g/liter, $KHCO_3$ 1 g/liter, EDTA 3.7 g/liter). The mixture was immediately subjected to centrifugation at 400g for 15 minutes at 20°C, and the pellets were collected. The pellets, which contained the remaining nucleated cells and debris, were resuspended in 3 ml of PBS, laid on top of a density barrier (density is 1.063), and subjected to centrifugation (360g for 15 minutes at 20°C), as diagramed in Figure 1A. This barrier was prepared by mixing 1 ml Opti-Prep (Sigma-Aldrich) with 4.4 ml of PBS. The resulting pellet, a collection of nucleated cells with density greater than 1.063, was resuspended in complete medium (α-minimal essential medium [MEM] with 20% fetal bovine serum [FBS], 1$\times$ antibiotic-antimycotic, 20 mg/liter gentamicin; all from Life Technologies) to produce the heavy fraction (HF) (Fig. 1).

Coculture System

The HF suspension was seeded on a Transwell insert (Corning, Corning, NY, http://www.corning.com) at a density of 1–1.5 $\times$ 10^5 cells per cm^2 in 1 ml of complete medium. The feeder cells were immortalized mouse hepatic, AML12 cells [17] that had been treated with mitomycin C (MMC) (Sigma-Aldrich), following the manufacturer's instructions. In brief, monolayers of AML12 cells were incubated with the complete medium containing MMC at a final concentration of 30 μg/ml. After 2 hours of incubation, the AML12 cells were washed twice with PBS, detached with trypsin-EDTA (0.5%), and resuspended in the complete medium. MMC-treated AML12 cells were then seeded on the polystyrene surface underneath the Transwell insert at a density of 5 $\times$ 10^4 cells per cm^2 in 2 ml of complete medium. The HF cells and MMC-treated AML12 cells were separated by a polyester

membrane (0.4 μm diameter pore size). No mixing of cells was observed during the course of our experiment. The coculture system was incubated at 37°C in a humidified CO_2 (5%) incubator. The medium was changed every 3 days, and the resultant cells on the Transwell inserts were harvested in 3–5 weeks. The cells produced in the Transwell membrane without further passage on tissue culture dishes were defined as at passage 0.

Flow Cytometry

To analyze the surface markers on the cells on the Transwell inserts, the cells were detached from the membrane using Accutase (Innovative Cell Technologies, San Diego, CA, http://www.accutase.com), resuspended in the complete medium, stained with fluorophore-conjugated monoclonal antibodies, and subjected to analysis using the BD LSRII analyzer (BD Biosciences, San Jose, CA, http://www.bdbiosciences.com). The antibodies used were anti-CD45/APC, anti-stem cell antigen 1 (Sca-1)/APC-Cy7, anti-lineage (Lin)/Pacific Blue, anti-c-kit/Pacific Blue, anti-c-kit/phycoerythrin (PE)-Cy7, anti-CD73/PE, anti-CD44/Alexa Fluor 700, anti-CD105/Pacific Blue, anti-CD105/Alexa Fluor 488, anti-CD140α/PE, anti-CD29/Pacific Blue, anti-CD90.1/PE, anti-CD90.1/PerCp-cy5.5, anti-CD19/Alexa Fluor 700, anti-CD14/PE-Cy7, anti-CD34/PE/Cy5 (purchased from BioLegend, San Diego, CA, http://www.biolegend.com), and anti-CD34/Alexa Fluor 700 (eBioscience Inc., San Diego, CA, http://www.ebioscience.com).

Purification of CD45$^-$ Cells Grown in the Coculture System

The CD45$^-$ subset of cells was purified by successive cell passages and magnetic-activated cell sorting (MACS). CD45$^-$ cells were found to detach relatively quickly from the Transwell membranes and culture dishes compared with CD45$^+$ cells. Highly enriched (up to 80% purity, as judged using flow cytometry) CD45$^-$ cells were obtained with a single passage. The resultant population of enriched CD45$^-$ cells was further subjected to depletion of CD45$^+$ cells using MACS MicroBead Technology (Miltenyi Biotec, San Diego, CA, http://www.miltenyibiotec.com). In brief, the cells were mixed with rat anti-mouse anti-CD45 (500 μg/ml) at a volume ratio of 1:100 in complete medium. After 40 minutes of incubation at 4°C with gentle rotation, the unbound anti-CD45 was removed by centrifugation, and goat anti-rat IgG MicroBeads were applied and incubated for another 40 minutes. The resultant cultures were passed through an LS column to deplete the CD45$^+$ cells, in accordance with the manufacturer's instructions, except that complete medium was used throughout. The flow through was cycled back to the column 5 times before obtaining the final flow through, which contained the CD45$^-$ cells. This process led to a high cell survival rate and near homogeneity of CD45$^-$ cells, determined using a live cell immunofluorescence assay. This cell population of purified CD45$^-$ cells was used for additional experiments.

Live Cell Immunofluorescence

To investigate the cell surface marker expression of living purified CD45$^-$ cells, 5,000 cells in 100 μl of complete medium were seeded per well in a 96-well plate (Corning) and incubated in a humidified CO_2 incubator. After 48 hours, the medium was replaced with 50 μl of fresh culture medium containing the primary antibody at the concentration of 5 μg/ml, and the culture plate was returned to the incubator. All primary antibodies were purchased from BioLegend. Except for anti-CD29 and anti-CD90.1, all antibodies
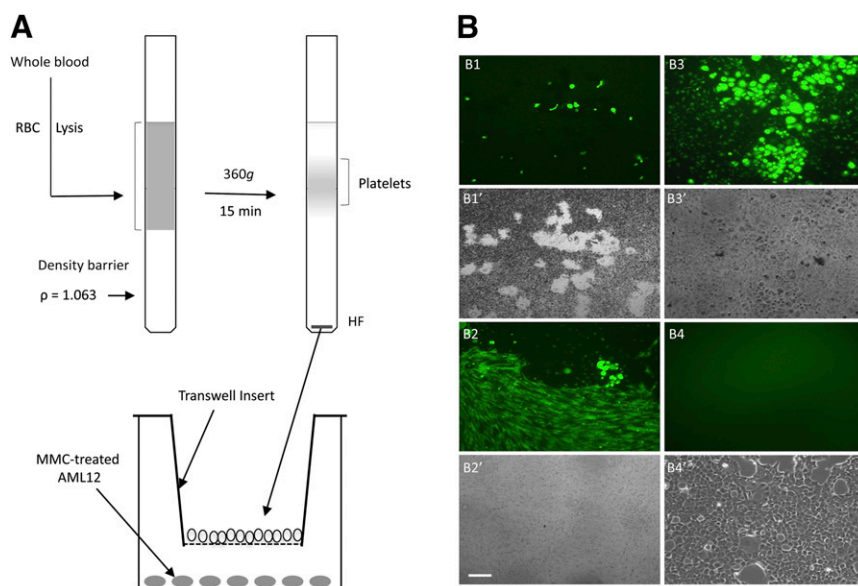
Figure 1. The coculture system and cells cultured from peripheral blood. **(A):** Design of the coculture system. Whole blood was subjected to RBC lysis and applied to an OptiPrep density barrier of buoyant density 1.063 ($\rho = 1.063$) for centrifugation. The resultant pellet, termed the "HF," was suspended in culture medium and seeded onto a 24-mm Transwell insert (polyester membrane, 0.4-μm pore size) at a density of $1-1.5 \times 10^5$ cells per cm^2 in 1 ml of medium. MMC-treated AML12 cells were seeded onto the polystyrene surface underneath the Transwell insert at a density of 5×10^4 cells per cm^2 in 2 ml of medium. **(B):** Cells on the Transwell inserts after 17 days of incubation. Cells appeared on the Transwell inserts in the absence **(B1, B1′)** and presence **(B2, B2′, B3, B3′)** of the feeder cells AML12. Scale bar = 90 μm. **(B4, B4′):** MMC-treated AML-12 cells attached onto the polystyrene culture dish underneath the Transwell insert. The cells on the Transwell inserts were recorded by photomicrography through the green fluorescent protein channel **(B1–B4)** and by phase-contrast microscopy **(B1′–B4′)**. The cells from **B2**, a population of cells that included fibroblastic cells, among the other cell types, were termed population 1 cells. The cells from **B3**, a population of cells that do not have fibroblastic cells were termed population 2 cells. Abbreviations: HF, heavy fraction; MMC, mitomycin C; RBC, red blood cell.

were rat-produced. Anti-CD29 was produced from the Armenian hamster and was conjugated with biotin. Anti-CD90.1 was produced from the mouse. After 40 minutes, the medium containing the primary antibody was removed. The cells were washed twice with fresh medium and were further incubated in 50 μl of fresh medium containing 4 μg/ml goat anti-rat IgG conjugated with Alexa Fluor 594 (Life Technologies), 0.2 μM Calcein AM (BD Biosciences, San Jose, CA), and 10 μg/ml Hoechst 33342 (Life Technologies). The detection of anti-CD29 was by streptavidin conjugated with Alexa Fluor 594 (Life Technologies). The detection of anti-CD90.1 was by goat anti-mouse IgG conjugated with Alexa Fluor 594 (Life Technologies). The cells were incubated for another 40 minutes, washed once with the normal medium, and incubated in 50 μl of the fresh medium without phenol red for microscopy (DMI 4000B microscope, Leica, Buffalo Grove, IL, http://www.leica.com). Normal rat IgG, biotin-conjugated Armenian hamster IgG, and normal mouse IgG were used as negative controls. Photomicrographs were taken, adjusted for their brightness and contrast, and merged using Adobe Photoshop CS5 (Adobe, San Jose, CA, http://www.adobe.com).

Osteogenic Differentiation Assay

Cells at $2-7 \times 10^4$ per well were seeded to a 2-cm^2 polystyrene well (Corning). After 48 hours, the cells were subjected to osteoblast differentiation medium (ODM; α-MEM containing 10% FBS, 1$\times$ penicillin-streptomycin, 0.1 μM dexamethasone, 10 mM β-glycerol phosphate, and 50 μM ascorbic acid) [18, 19]. The cells were cultured in ODM for 14 days, with medium changes every 2 days. Alizarin red S (Sigma-Aldrich) was used to stain the accumulated calcium deposits. In brief, the cells were fixed with 10% neutral buffered formalin, stained with alizarin red staining solution

(0.2% alizarin red in deionized H$_2$O with pH adjusted by 15 N ammonium hydroxide to 6.4) for 30 minutes at room temperature, and washed 3 times with PBS before microscopy. For quantitative measurement of calcium deposition, duplicate experiments were performed, in which alizarin red S was extracted with 1 ml of solution containing 20% methanol and 10% acetic acid. The resulting clear yellow solution was quantitated by optical density (OD)$_{405}$ measured using a UV-visible spectrometer (Pharmacia Ultrospec 2100 pro).

Adipogenic Differentiation Assay

Purified CD45$^-$ cells (passage 2) were seeded at 2×10^4 cells per 2-cm^2 polystyrene well. After 48 hours, the cells were subjected to adipocyte differentiation medium (ADM): α-MEM containing 10% FBS, 1$\times$ penicillin-streptomycin, 0.5 μM dexamethasone, 0.5 μM 3-isobutyl-1-methylxanthine, and 50 μM indomethacin [20]. The cells were cultured in ADM for 14 days, with medium changes every 2 days, and subjected to detection of lipid droplets accumulation by Oil Red O (Sigma-Aldrich) staining. In brief, the cells were fixed with 10% neutral buffered formalin, washed in PBS, stained with Oil Red O staining solution (3 parts Oil Red O stock solution and 2 parts PBS) for 10 minutes at room temperature, followed by washing twice with PBS.

Chondrogenic Differentiation Assay

Purified CD45$^-$ cells (passage 2) were induced toward chondrogenesis using the Completed StemXVivo Chondrogenic Differentiation Medium (R&D Systems, Minneapolis, MN, http://www.rndsystems.com). In brief, 1.25×10^5 cells were washed once with the base medium, resuspended in 0.5 ml of the differentiation

medium in a 15-ml conical centrifugation tube (BD Falcon, San Jose, CA), and subjected to centrifugation at 200g for 5 minutes at room temperature. The resultant cell pellets, together with the centrifugation tube and differentiation medium, were moved to a humidified CO_2 incubator for 3 weeks, with medium changes every 3 days. The micromass formed was fixed with 4% paraformaldehyde, embedded with Tissue-Tek OCT (Sakura Finetek USA, Inc., Torrance, CA, http://www.sakura-americas.com), sectioned with microtone, and stained with Alcian blue (Sigma-Aldrich), which stains glycosaminoglycans in cartilage. Nuclear fast red staining (Vector Laboratory, Burlingame, CA, http://www.vectorlabs.com) was also performed to stain the nucleus.

Transplantation of Population 1 Cells to Calvarial Bone Defects

All experiments were performed in accordance with the Stanford University Animal Care and Use Committee guidelines (protocol ID no. 9999). Female athymic CD-1 nude mice (Charles River Laboratories), aged 8 to 10 weeks, were housed 5 per cage in autoclaved cages with a 12-hour light/dark cycle and provided standard food and water ad libitum. One week before calvarial defect creation, their food was changed to a diet that included Uniprim antibiotic (Harlan Laboratories, Indianapolis, IN, http://www.harlan.com). The calvarial defect procedure was performed as previously described by Gupta et al. [21]. The population 1 (pop1) cells (from CD-1 mice), which had been cultured in our coculture system for 5 weeks without further passage (passage 0), were seeded onto hydroxyapatite-poly(lactic-coglycolic acid) (HA-PLGA) scaffolds in the complete medium as described and incubated at 5% CO_2 at 37°C for 24 hours. After creation of 4-mm (critical size) calvarial defects on the right parietal bone, the pop1 cell-seeded HA-PLGA scaffolds or control unseeded HA-PLGA scaffolds were gently washed in PBS and placed into the defect. The scalp was immediately closed with interrupted 7-0 Vicryl sutures (Ethicon, Somerville, NJ, http://www.ethicon.com), and the mice were allowed to recover, as previously described [21]. Quantitative bone analysis was performed immediately after surgery and at weeks 2, 4, 6, and 8 by microcomputed tomography (micro-CT) using the eXplore RS Micro-CT system (GE Healthcare, Little Chalfont, U.K., http://www.gehealthcare.com) at 45 μm resolution. The Student t test was used for statistical analysis, and p values $<$ .05 were considered statistically significant. Three-dimensional micro-CT images were reconstructed using native software, and the defect size was quantified using Adobe Photoshop CS6 (Adobe).

RESULTS

Production of Putative Stem Cells and Progenitor Cells From the Coculture System

We designed a coculture system (Fig. 1A) based on AML12 cells, a mouse hepatic cell line [17]. AML12 cells were chosen because of their ability to function as feeder cells for stem cell maintenance in vitro [22–24]. Using a 1.063 density barrier, the nucleated cell fraction, termed the "heavy fraction" (HF), was isolated from the peripheral blood of FVB-L2G mice. These mice expressed a fusion protein of luciferase and GFP in all cells. The HF was seeded on Transwell inserts at a density of $1–1.5 \times 10^5$ cells per cm^2 and cocultured with mitomycin C-treated AML12 cells in a system in which both groups were separated (Fig. 1A). When no AML12 cells were
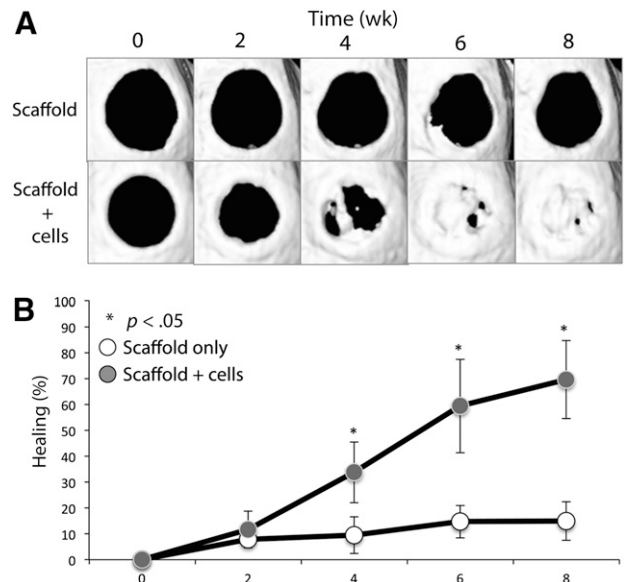

Figure 2. Peripheral blood-derived cells heal critical-sized calvarial bone defects. One half of 1 million population 1 (pop1) cells, derived from CD-1 mouse peripheral blood, were seeded onto a hydroxyapatite-poly (lactic-coglycolic acid) scaffold and transplanted onto a critical-sized calvarial defect created in athymic CD-1 nude mice. **(A):** Healing of calvarial defects was monitored using microcomputed tomography. **(B):** Quantitation of the healing process monitored in **(A)**. The filled circles represent transplantation with scaffold seeded with cells, and the open circles represent transplantation with scaffold alone. The p value is $<$ .05 indicating statistical significance. The defects only healed when treated with pop1 cells.

seeded as a control, very few or no cells appeared on the Transwell inserts (Fig. 1B1) during the course of the experiment. However, in the presence of AML12 cells, many cells appeared on every Transwell insert after 1–2 weeks of incubation, indicating the supportive effect from the AML12 cells. The cells on the Transwell inserts included small star-shaped cells and round cells (Fig. 1B2, 1B3). Unexpectedly, relatively large fibroblast-like cells were found on some of the Transwell inserts in the presence of AML12 cells (Fig. 1B2). Transwell inserts with these fibroblastic cells, among the other cells, were termed the population 1 group or pop1 group. Transwell inserts that did not have fibroblastic cells (Fig. 1B3) were termed the population 2 group or pop2 group. The green fluorescence of these cells demonstrated that they were all derived from the peripheral blood of FVB-L2G mice rather than from the AML12 cells, which do not express GFP (Fig. 1B4). The fibroblastic cells of the pop1 group (Fig. 1B2) quickly proliferated, resulting in confluence in another 2 weeks. The morphology and highly proliferative nature of these fibroblastic cells are reminiscent of the properties of stromal stem cells.

Repair of Calvarial Bone Defects

To evaluate the regenerative capability of the cells in the pop1 group, the highly reproducible in vivo critical-sized calvarial bone defect model was used [2, 21, 25]. One half of 1 million cells were seeded onto a HA-PLGA scaffold. The cell-seeded scaffolds were transplanted into a 4-mm diameter (critical-sized) defect in parietal calvarial bone. Untreated, calvarial bone defects of this size will not heal. Bone regeneration was quantified using micro-CT over the course of 8 weeks (Fig. 2A). As shown in Figure 2B, defects treated with pop1 cell-seeded scaffolds healed at a faster rate than those treated with unseeded control scaffolds. This

was evident as early as 4 weeks, with 33.76% healing with the pop1 cell-treated calvarial defects versus 9.47% in the controls ($p < .05$). At 6 weeks, defects treated with pop1 cells had 59.41% osteogenesis compared with 14.68% in those treated with scaffold alone ($p < .05$). This trend continued through week 8, when healing was found to be 69.65% in pop1 cell-seeded scaffolds and 14.94% in unseeded control scaffolds ($p < .05$). Therefore, treatment with pop1 cells significantly increased osteogenesis and bone regeneration in critical-sized calvarial defects.

Osteogenic Differentiation Potential of CD45⁻ Cells

Knowing that multiple cell types exist in pop1, we next questioned which subset is responsible for repairing the calvarial bone defects. We first determined the surface marker profile of the pop1 cells with flow cytometry. As shown in Figure 3A, a population of CD45⁺ cells was identified. This finding was expected, because CD45 is a surface marker associated with all hematopoietic cells, except red blood cells and platelets. Importantly, a population of potentially nonhematopoietic cells that were negative or weakly positive for CD45 expression was also found (Fig. 3A). To determine which population of cells was responsible for healing the calvarial defects, we tested the in vitro osteogenic differentiation activity of CD45⁻ and CD45⁺ cells. This activity represents a unique property of osteoblasts (committed bone precursor cells): cellular mineralization (mostly calcification) in response to differentiation signals such as β-glycerol phosphate [18]. The calcium deposit can be stained with alizarin red S and quantified at OD_{405}, which has a linear range between 0 and 2.5 [26].

CD45⁻ cells were purified to near homogeneity from pop1 at passage 2 and subjected to differentiation induction by ODM. As shown in Figure 4A1, a high level of matrix calcification with purified CD45⁻ cells was observed. Therefore, the CD45⁻ cells have the intrinsic capability of osteogenic differentiation. We next determined the contribution of CD45⁻ cells to the overall calcification activity of the pop1 cells. Pop1 cells were fractionated by MACS into 2 groups of cells containing different proportions of CD45⁻ cells. One group contained 19% CD45⁻ cells (Fig. 4B2, 4B3) and the other contained 60% CD45⁻ cells (Fig. 4B5, 4B6). Equal amounts (6.7×10^4) of cells from each group were seeded, and an in vitro osteogenic differentiation assay was performed (Fig. 4B1, 4B4). As shown in Figure 4C, ODM induction of the group with 19% CD45⁻ cells resulted in an average of 0.65 U of OD_{405}. Induction of the group with 60% CD45⁻ cells resulted in an average of 1.7 U of OD_{405}. Therefore, an increase in the proportion of CD45⁻ cells, with a decrease in CD45⁺ cells, resulted in an increase in calcification activity (i.e., threefold increase of CD45⁻ cells resulted in an approximately 2.6-fold increase of OD_{405}). These data indicate that CD45⁻ cells are the primary cells responsible for the calcification activity in the pop1 group. CD45⁺ cells only contributed very minor calcification activity. The intrinsic minor osteogenic differentiation activity of CD45⁺ cells is presented in supplemental online Figure 1. We therefore hypothesized that CD45⁻ cells are most likely responsible for healing the calvarial bone defects.

Surface Marker Profile of CD45⁻ Cells

To establish the identity of the CD45⁻ cells isolated from pop1, we examined their morphology and surface marker profile. As shown in Figure 5A, the purified CD45⁻ cells displayed a multipole
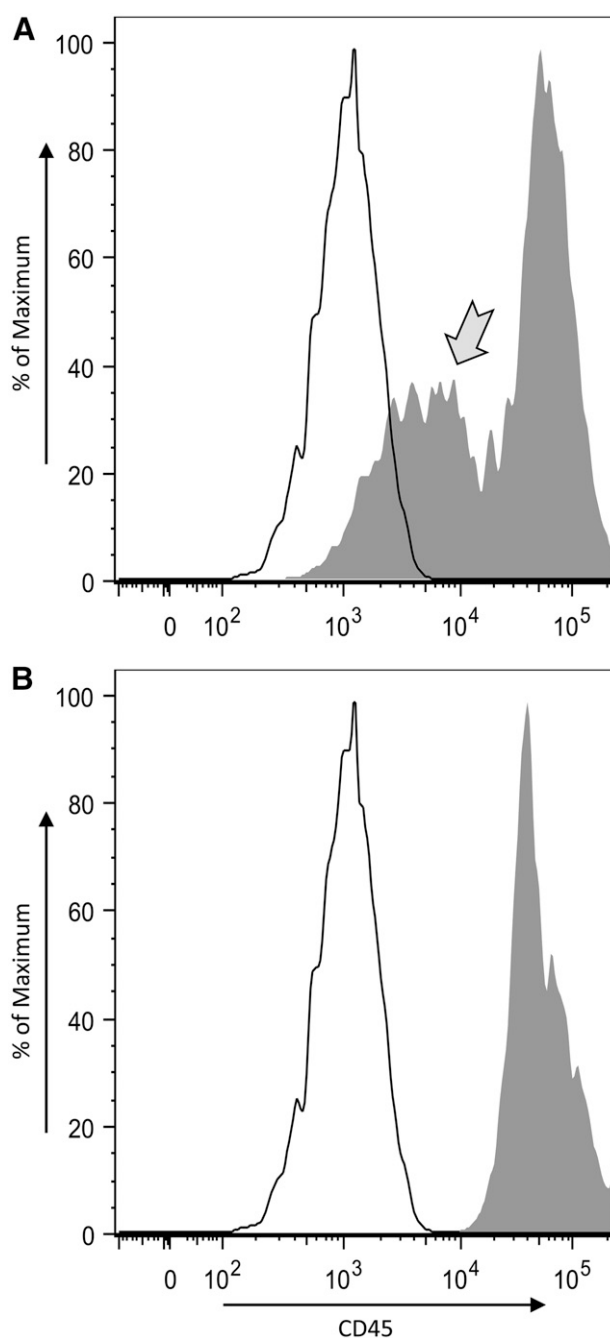

Figure 3. Flow cytometry analysis of CD45 expression on population 1 (pop1) cells. Peripheral blood from FVB luciferase-green fluorescent protein mice was processed and cultured in the coculture system for 5 weeks. Cells on the Transwell inserts were detached and stained (gray area) or not stained (light area) with anti-CD45/APC followed by flow cytometry. **(A):** Staining result of pop1 cells, a cell population from Transwell inserts that have fibroblastic cells among other cells. The subset of cells that were negative or weakly positive for CD45 expression is shown with an arrowhead. **(B):** Staining result of population 2 cells, cells from the Transwell inserts without fibroblastic cells.

fibroblastic morphology, implicating a stromal cell phenotype. The CD45⁻ fibroblastic cells were all positive for Sca-1, a surface marker frequently associated with stem and progenitor cells [27]. The CD45⁻ cells were further analyzed using flow cytometry for the expression of surface markers Lin (major hematopoietic cell
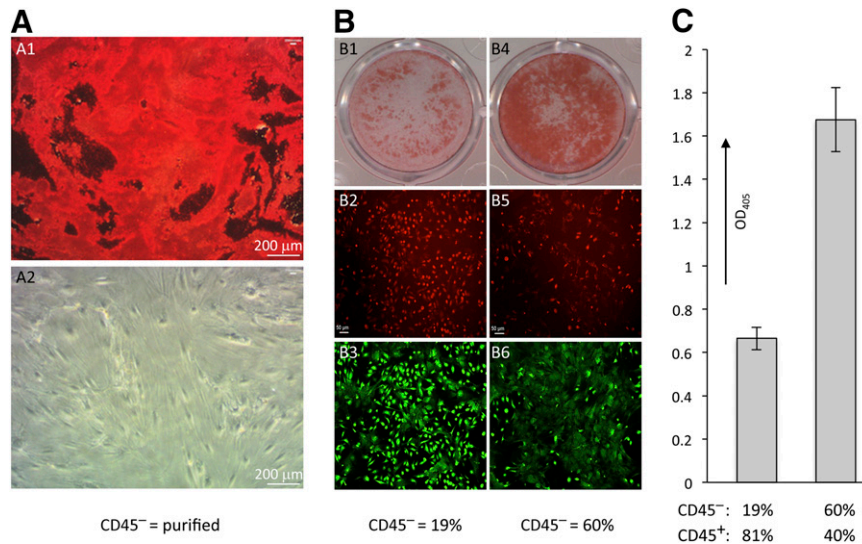
Figure 4. In vitro osteogenic differentiation activity of the CD45⁻ subset of cells from population 1 (pop1). **(A):** Purified CD45⁻ cells (pop1, passage 2, derived from FVB luciferase-green fluorescent protein mice) were cultured in osteogenic differentiation medium **(A1)** or in normal growth medium **(A2)** for 2 weeks. The red color represents calcium deposits stained by alizarin red S. Scale bars = 200 μm. **(B):** Determination of the CD45⁻ cell proportion in two populations of cells fractionated from pop1 cells by anti-CD45 coupled with magnetic beads. **(B2):** Cells from one population were stained with rat anti-mouse CD45 (coupled with goat anti-rat Alexa Fluor 594) to determine the number of CD45⁺ cells (in red). Scale bar = 50 μm. **(B3):** The same cells shown in **(B2)** were also stained with calcein AM to determine the total number of metabolically active cells (in green). The endogenous green fluorescence intensity in each cell was too weak to be visible. The proportion of CD45⁻ cells of this population was calculated to be 19% (i.e., 81% of CD45⁺ cells). Likewise, an aliquot of cells from another population was stained with anti-CD45 (scale bar = 50 μm) **(B5)** and calcein AM **(B6)** and was calculated to contain 60% of CD45⁻ cells (i.e., 40% of CD45⁺ cells). **(C):** In vitro osteogenic differentiation activity of the populations of 19% and 60% of CD45⁻ cells. The results were derived from duplicated experiments, in which 6.7 × 10⁴ cells from each population were seeded for an in vitro osteogenic differentiation assay. A representative result for each population is shown in **B1** (19% of CD45⁻ cells) and **B4** (60% of CD45⁻ cells). The measurement of osteogenic differentiation activity at OD₄₀₅ was performed as described in Materials and Methods. The amount of osteogenic activity of each population correlated with the amount of CD45⁻ cells in each. Abbreviation: OD₄₀₅, optical density 405.

lineages markers, including CD11b, CD3e, CD45R/B220, TER-119 and Ly-6G/Ly-6c), CD19, c-kit, CD34, CD90.1, CD73, CD105, CD44, CD29, CD140α, and CD106. As shown in Figure 5B, the CD45⁻ cells were negative for Lin and CD19. They were also negative for c-kit and CD34, markers associated with hematopoietic stem cells. However, the CD45⁻ cells were positive for CD90.1, CD73, CD105, CD44, CD29, CD140α, and CD106. Taken together, the CD45⁻ cells are a population of nonhematopoietic cells. The expression of CD105, CD73, and CD90 and the lack of expression of CD45, CD34, CD11b, and CD19 are among the minimal criteria for multipotent MSCs, as defined by the ISCT [28]. Moreover, the expression of CD44, CD106, and CD140α was previously reported for bone marrow-derived MSCs [29–32] (Table 1). Therefore, these CD45⁻ fibroblast-like cells have the surface marker profile of MSCs and are very likely a type of mesenchymal stem cell.

Trilineage Differentiation

According to the ISCT, cells defined as MSCs are capable of trilineage differentiation (i.e., osteogenic, adipogenic, and chondrogenic). We first demonstrated the osteogenic differentiation capability of our CD45⁻ cells (Fig. 4). We next examined their capabilities for chondrogenic and adipogenic differentiation. As shown in Figure 6A, when the purified CD45⁻ cells were subjected to chondrocyte differentiation medium, a micromass was found that stained positively with Alcian blue, which stains glycosaminoglycans, indicating chondrogenic differentiation [20]. When the cells were subjected to adipocyte differentiation medium, oil droplets inside the cells were observed that stained positively

with Oil Red O (Fig. 6B), indicating adipogenic differentiation [20]. Therefore, together with the osteogenic differentiation capability shown in Figure 4, these CD45⁻ fibroblastic cells possess the capability of trilineage differentiation. These data support the conclusion that the fibroblastic CD45⁻ cells fulfill the minimal criteria of MSC definition proposed by the ISCT. In view of their peripheral blood origin, we named the cells, blood-derived mesenchymal stem cells or BD-MSCs.

DISCUSSION

Stomal cells capable of repairing critical-sized bone defects have previously been isolated from bone marrow [1] and adipose tissue [2]. These cells are isolated using invasive procedures, such as bone marrow aspiration and liposuction. Cells with similar potential, but retrieved from peripheral blood, will provide an advantageous alternative source owing to their ease of retrieval. Circulating cells with intrinsic osteogenic function have been described in other models. Kuznetsov et al. [14] reported that transplantation of circulating skeletal stem cells to the subcutaneous pockets of mice resulted in bone formation, indicating intrinsic osteogenic differentiation potential. Wan et al. [16] reported that a group of undefined allogeneic peripheral blood-derived MSC-like cells improved healing of critical-sized ulna bone defects in rabbits. We have extended these previous findings and demonstrated that a population of mouse peripheral blood-derived cells isolated and expanded by our coculture system, termed pop1 cells, can enhance healing of mouse calvarial bone defects. Ulna bone formation and calvarial bone formation represent the two
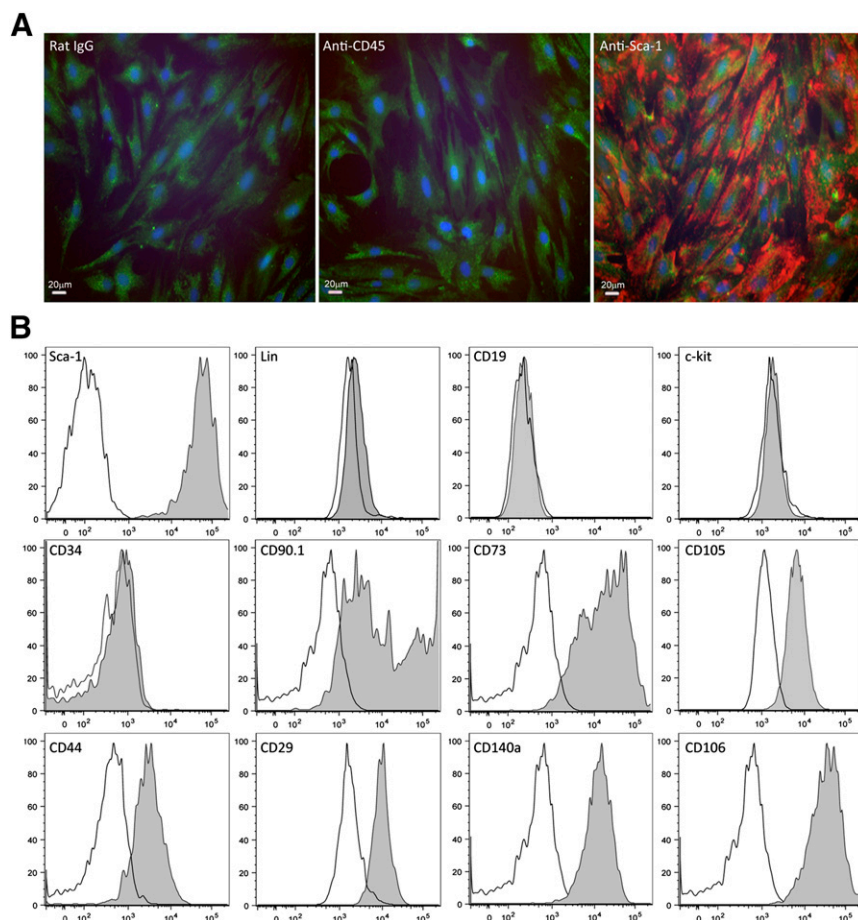
Figure 5. Surface marker analysis of the CD45⁻ cells from population 1 (pop1). **(A):** Live cell immunofluorescence assay of CD45⁻ cells (passage 2) that were purified to near homogeneity from pop1 (derived from FVB luciferase-green fluorescent protein mice). The red color indicates surface markers specified for investigation. The blue color represents nuclei stained by Hoechst 33342. The green color represents the cytoplasm of metabolically active cells stained by calcein AM. Rat IgG was used as a negative control for all primary antibodies. Scale bars = 20 μm. **(B):** Multicolor flow cytometry was performed to analyze the surface markers of CD45⁻ cells enriched by the cell passage procedure. The CD45⁻ cells were gated and analyzed for the expression of Sca-1, Lin, CD19, c-kit, CD34, CD90.1, CD73, CD105, CD44, CD29, CD140, and CD106. Cells analyzed for CD19 and CD105 were from pop1 at passage 1. Cells for remainder of the experiments were from pop1 at passage 2. The light areas indicate unstained cells and the gray areas represent cells stained by antibody against specified antigens. The X-axis represents intensity of the signal while the Y-axis represents percentage of maximum cell number. Abbreviations: Lin, lineage; Sca-1, stem cell antigen 1.

major bone formation modes: endochondral ossification and intramembranous ossification, respectively [33, 34]. The present study has thus provided a proof of principle of treating bone defects with peripheral blood-derived cells. We have further discovered that, among pop1 cells, the most plausible candidate cell responsible for healing the critical-sized calvarial defects is a group of CD45⁻ fibroblastic cells. These are the cells predominantly responsible for the calcification activity of pop1 cells. Calcification activity is unique to osteoblasts and also is an essential process during bone formation [18]. We eventually identified the CD45⁻ fibroblastic cells as a type of MSCs, named BD-MSCs, on the basis of their surface marker profile and their trilineage differentiation potential, as defined by the ISCT. BD-MSCs differ from the circulating skeletal stem cells described by Kuznetsov et al. [14] because the latter do not express CD105, a critical surface marker for MSC determination. In contrast, Wan et al. [16] described a group of peripheral blood-derived cells capable of healing rabbit critical-sized ulna bone defects as MSCs. However, BD-MSCs cannot be compared with those cells because the surface marker profile for the latter is not available.

Many reports and reviews have discussed MSCs in peripheral blood using various animal models [7, 9–11, 35]. However, because of the lack of a standard set of criteria for MSC definition in most reports, a conclusive comparison between BD-MSCs and previously described cells is impractical. The ISCT has defined a set of minimal criteria to address this issue for human MSCs [28]. According to the ISCT, human MSCs must fulfill these minimal criteria: they must be plastic adherent, express surface markers CD105, CD73, and CD90 and lack expression of CD45, CD34, CD14 or CD11b, CD79α or CD19, and human leukocyte antigen-DR (for human cells), and be capable of differentiation toward osteoblasts, adipocytes, and chondrocytes. BD-MSCs, although derived from mouse peripheral blood, fulfill these criteria defined for human MSCs. However, the surface marker profiles or differentiation phenotypes of previously described peripheral blood MSCs only partially fulfilled [14, 16, 36–43] or, in some studies, deviated from the ISCT criteria [44]. Therefore, determining whether BD-MSCs and these previously reported cells are related is not possible. Because of reproducibility issues [45–47], the existence of MSCs in the peripheral blood is still questioned. From

Table 1. Surface markers of BD-MSCs, MSCs defined by ISCT, and MSCs isolated from mouse bone marrow

Marker	BD-MSC	ISCT MSC [28]	Mouse BM-MSC
CD45	−	−	−/+ [30]
CD34	−	−	−/+ [30]
CD11b	−	−	− [31]
CD19	−	−	− [31]
Lin	−		
c-Kit	−		−/+ [30]
CD105	+	+	+ [30]
CD73	+	+	−/+ [30]
CD90.1	+	+	−/+ [30]
Sca-1	+		+ [29, 30]
CD44	+		+ [30]
CD29	+		+ [30]
CD106	+		+ [32]
CD140	+		+ [29]

Abbreviations: +, expression; −, no expression; −/+, reports of both expression and no expression; BD-MSC, blood-derived mesenchymal stem cells; ISCT, International Society for Cellular Therapy; Mouse BM-MSC, bone marrow mesenchymal stem cells isolated from mouse; MSCs, human mesenchymal stem cells; Sca-1, stem cell antigen 1.

this perspective, BD-MSCs provide new evidence that MSCs, as defined by the ISCT, can be cultured and expanded from the peripheral blood.

The question of whether BD-MSCs exist in the circulation or are a result of our unique coculture condition is important. In order to answer this question, freshly isolated peripheral blood cells were subjected to flow cytometry to examine cells that simultaneously express the characteristic BD-MSC surface markers (CD45$^{−/weak}$, CD19$^−$, CD34$^−$, lin$^−$, Sca-1$^+$, CD105$^+$, CD73$^+$, and CD90.1$^+$). Our analysis indicated the nonexistence or a very small number (0.0019% or 20 cells per 10^6 nucleated cells) of circulating BD-MSCs (supplemental online Fig. 2), which is too rare to prove existence. Thus, the existence of circulating BD-MSCs cannot be fully demonstrated. The BD-MSCs might exist in the circulation in very low numbers or be the result of cultivation of origin cells of BD-MSCs, which do not express all the characteristic BD-MSC surface markers, in the circulation with our unique culture conditions.

A key to the successful culture of BD-MSCs from the peripheral blood is our coculture system, in which nonreplicating hepatic lineage (AML12) cells were present as feeder cells. AML12 cells were used because hepatic cells are known to produce the cytokines frequently used for stem cell culture [22–24]. Without the presence of AML12 cells, few or no cells appeared on the Transwell inserts (Fig. 1B1). In the presence of AML12 cells, vigorous cell proliferation on the Transwell inserts was observed (Fig. 1B2, 1B3), indicating that the factors secreted from AML12 cells facilitated proliferation of the peripheral blood-derived cells. However, even with the support of AML12 cells, our coculture system produces BD-MSCs in 1–4 of the Transwell inserts in a 6-well format seeded with 2.9×10^6 nucleated HF cells. This frequency is low but comparable to MSCs obtained from the bone marrow (1 from 10^6 nucleated bone marrow cells) [35]. Nevertheless, this frequency might not reflect their in vivo abundance, because it is condition dependent. For example, we have observed that serum starvation of AML12 cells can increase BD-MSC culture
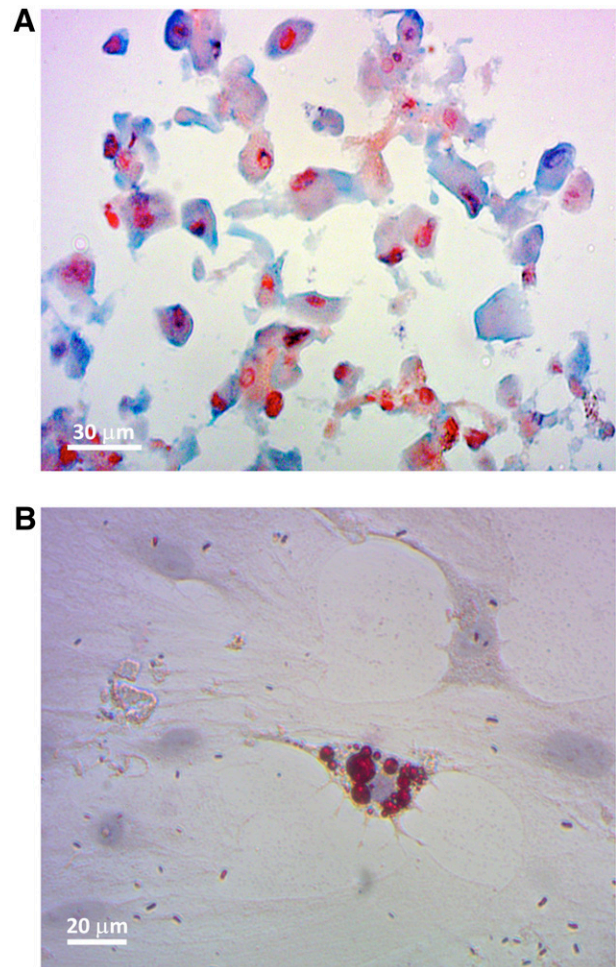
Figure 6. Chondrogenic and adipogenic differentiation of CD45$^−$ cells derived from peripheral blood. **(A):** Purified CD45$^−$ cells (population 1 [pop1], passage 2) were subjected to chondrogenic differentiation. The blue color represents glycosaminoglycans stained by Alcian blue, indicating chondrogenic differentiation. The red color represents nuclei stained red by nuclear fast red. Scale bar = 30 μm. **(B):** Purified CD45$^−$ cells (pop1, passage 2) were subjected to adipogenic differentiation. The red color represents staining of lipid droplets by Oil Red O, indicating adipogenic differentiation. Scale bar = 20 μm. The peripheral blood-derived CD45$^−$ cells exhibited both chondrogenic differentiation and adipogenic differentiation.

frequency more than four times from age- and sex-matched mice (data not shown). Therefore, our current coculture system is likely not the most optimized growth condition. Identification of AML12-released factors that facilitate cell proliferation might be the key to enhancing BD-MSC isolation. Transforming growth factor-α, insulin-like growth factor 1, hepatocyte growth factor, and vascular endothelial growth factor, four well-recognized cytokines produced by hepatocytes, were individually tested and were insufficient to stimulate proliferation of peripheral blood cells (data not shown). Interestingly, although the heavy fraction cells can be stimulated to produce BD-MSCs in our coculture system, freshly isolated CD45$^−$/CD19$^−$/CD11b$^−$ cells from the circulation could not be stimulated to produce BD-MSCs in the same coculture system. This population of cells exhibits a subset of the BD-MSC surface marker profile and contains origin cells of BD-MSCs or circulating MSCs. A combination of AML12 cells and all cell types in the HF are required for BD-MSC production (supplemental online Fig. 3) from this

population of cells. The stimulation by AML12 cells could therefore be indirect and act through non-BD-MSC cells.

Recently Guihard et al. [48] reported that activated monocytes/macrophages (isolated as CD14^{+} cells) greatly stimulated the calcification activity of bone marrow-derived MSCs through oncostatin M signaling. Nicolaidou et al. [49] also reported that monocytes promote MSC osteoblast formation through activating signal transducer and activator of transcription 3, a positive feedback regulator for oncostatin M signaling. These findings suggest that during the bone healing process, the osteogenic differentiation activity of MSCs is regulated by other cells. We have demonstrated that cells from pop1, a mixture of BD-MSCs and CD45^{+} cells, can heal critical-sized calvarial defects. BD-MSCs are the predominant cells responsible for pop1 cells' calcification activity. However, the roles of the CD45^{+} cells, which are mostly CD14^{+} (data not shown), remain to be determined. Moreover, greater analysis of pop1 cells and BD-MSC cells in other MSC functional assays, such as ectopic bone organ formation [50], will be important to determine the specific functions of distinct MSC cell populations. Future studies on the interactions between BD-MSCs and cells in the bone wound will also provide valuable insights into the mechanisms underlying enhanced bone healing. An understanding of these mechanisms might result in the development of BD-MSC-based cell therapy to enhance bone repair.

CONCLUSION

We present a novel technique to isolate a population of cells derived from peripheral blood that enhance healing of calvarial bone defects. The BD-MSC is the most probable candidate cell responsible for the improved healing owing to its high cell calcification activity in response to osteogenic differentiation. BD-MSCs, which fulfill the MSC criteria as defined by the ISCT, provide new evidence that MSCs can be isolated and expanded from peripheral blood. The BD-MSC is an ideal cell type for the development of cell-based therapy to enhance bone repair.

AUTHOR CONTRIBUTIONS

S.L., M.S., and M.H.: conception and design; K.-J.H., J.-C.W., and M.S.H.: conception and design, collection and assembly of data, manuscript writing; M.T.L.: manuscript writing, financial support, administrative support; H.P.L: conception and design, financial support, manuscript writing, final approval of manuscript.

DISCLOSURE OF POTENTIAL CONFLICTS OF INTEREST

The authors indicated no potential conflicts of interest.

REFERENCES

1 Undale AH, Westendorf JJ, Yaszemski MJ et al. Mesenchymal stem cells for bone repair and metabolic bone diseases. Mayo Clin Proc 2009;84:893–902.

2 Cowan CM, Shi Y-Y, Aalami OO et al. Adipose-derived adult stromal cells heal critical-size mouse calvarial defects. Nat Biotechnol 2004;22:560–567.

3 Körbling M, Freireich EJ. Twenty-five years of peripheral blood stem cell transplantation. Blood 2011;117:6411–6416.

4 Psaltis PJ, Harbuzariu A, Delacroix S et al. Resident vascular progenitor cells—Diverse origins, phenotype, and function. J Cardiovasc Transl Res 2011;4:161–176.

5 Charbord P. Bone marrow mesenchymal stem cells: Historical overview and concepts. Hum Gene Ther 2010;21:1045–1056.

6 Bianco P, Robey PG, Saggio I et al. "Mesenchymal" stem cells in human bone marrow (skeletal stem cells): A critical discussion of their nature, identity, and significance in incurable skeletal disease. Hum Gene Ther 2010;21:1057–1066.

7 Hass R, Kasper C, Böhm S et al. Different populations and sources of human mesenchymal stem cells (MSC): A comparison of adult and neonatal tissue-derived MSC. Cell Commun Signal 2011;9:12.

8 da Silva Meirelles L, Chagastelles PC, Nardi NB. Mesenchymal stem cells reside in virtually all post-natal organs and tissues. J Cell Sci 2006;119:2204–2213.

9 Zhang Y, Huang B. Peripheral blood stem cells: Phenotypic diversity and potential clinical applications. Stem Cell Rev 2012;8:917–925.

10 He Q, Wan C, Li G. Concise review: Multipotent mesenchymal stromal cells in blood. STEM CELLS 2007;25:69–77.

11 Roufosse CA, Direkze NC, Otto WR et al. Circulating mesenchymal stem cells. Int J Biochem Cell Biol 2004;36:585–597.

12 Choi YH, Burdick MD, Strieter RM. Human circulating fibrocytes have the capacity to differentiate osteoblasts and chondrocytes. Int J Biochem Cell Biol 2010;42:662–671.

13 Kuwana M, Okazaki Y, Kodama H et al. Human circulating CD14+ monocytes as a source of progenitors that exhibit mesenchymal cell differentiation. J Leukoc Biol 2003;74:833–845.

14 Kuznetsov SA, Mankani MH, Gronthos S et al. Circulating skeletal stem cells. J Cell Biol 2001;153:1133–1140.

15 Eghbali-Fatourechi GZ, Lamsam J, Fraser D et al. Circulating osteoblast-lineage cells in humans. N Engl J Med 2005;352:1959–1966.

16 Wan C, He Q, Li G. Allogenic peripheral blood derived mesenchymal stem cells (MSCs) enhance bone regeneration in rabbit ulna critical-sized bone defect model. J Orthop Res 2006;24:610–618.

17 Wu JC, Merlino G, Fausto N. Establishment and characterization of differentiated, nontransformed hepatocyte cell lines derived from mice transgenic for transforming growth factor alpha. Proc Natl Acad Sci USA 1994;91:674–678.

18 Ecarot-Charrier B, Glorieux FH, van der Rest M et al. Osteoblasts isolated from mouse calvaria initiate matrix mineralization in culture. J Cell Biol 1983;96:639–643.

19 Li S, Quarto N, Longaker MT. Activation of FGF signaling mediates proliferative and osteogenic differences between neural crest derived frontal and mesoderm parietal derived bone. PLoS One 2010;5:e14033.

20 Pittenger MF, Mackay AM, Beck SC et al. Multilineage potential of adult human mesenchymal stem cells. Science 1999;284:143–147.

21 Gupta DM, Kwan MD, Slater BJ et al. Applications of an athymic nude mouse model of nonhealing critical-sized calvarial defects. J Craniofac Surg 2008;19:192–197.

22 Hepatocytes. Available at: http://www.copewithcytokines.de/cope.cgi?key=hepatocytes. Accessed December 16, 2014.

23 Growth Factors and Cytokines for Stem Cell Biology. Available at: http://www.sigmaaldrich.com/content/dam/sigma-aldrich/docs/Sigma-Aldrich/Brochure/1/growth_factors_and_cytokines.pdf. Accessed December 16, 2014.

24 Soto-Gutiérrez A, Navarro-Alvarez N, Zhao D et al. Differentiation of mouse embryonic stem cells to hepatocyte-like cells by coculture with human liver nonparenchymal cell lines. Nat Protoc 2007;2:347–356.

25 Lo DD, Hyun JS, Chung MT et al. Repair of a critical-sized calvarial defect model using adipose-derived stromal cells harvested from lipoaspirate. J Vis Exp 2012;(68):e4221.

26 Gregory CA, Gunn WG, Peister A et al. An alizarin red-based assay of mineralization by adherent cells in culture: Comparison with cetylpyridinium chloride extraction. Anal Biochem 2004;329:77–84.

27 Batts TD, Machado HL, Zhang Y et al. Stem cell antigen-1 (sca-1) regulates mammary tumor development and cell migration. PLoS One 2011;6:e27841.

28 Dominici M, Le Blanc K, Mueller I et al. Minimal criteria for defining multipotent mesenchymal stromal cells. The International Society for Cellular Therapy position statement. Cytotherapy 2006;8:315–317.

29 Houlihan DD, Mabuchi Y, Morikawa S et al. Isolation of mouse mesenchymal stem cells on the basis of expression of Sca-1 and PDGFR-α Nat Protoc 2012;7:2103–2111.

30 Boxall SA, Jones E. Markers for characterization of bone marrow multipotential stromal cells. Stem Cells Int 2012;2012:975871.

31 Sung JH, Yang HM, Park JB et al. Isolation and characterization of mouse mesenchymal stem cells. Transplant Proc 2008;40:2649–2654.

32 Qian H, Le Blanc K, Sigvardsson M. Primary mesenchymal stem and progenitor cells from bone marrow lack expression of CD44 protein. J Biol Chem 2012;287:25795–25807.

33 Bradley EW, McGee-Lawrence ME, Westendorf JJ. Hdac-mediated control of endochondral and intramembranous ossification. Crit Rev Eukaryot Gene Expr 2011;21:101–113.

34 Mackie EJ, Tatarczuch L, Mirams M. The skeleton: A multi-functional complex organ: The growth plate chondrocyte and endochondral ossification. J Endocrinol 2011;211:109–121.

35 Coutu DL, Francois M, Galipeau J. Regenerative Therapy Using Blood-Derived Stem Cells. In: Allan DS Strunk D, eds. Stem Cell Biology and Regenerative Medicine. Totowa, NJ: Humana Press, 2012:35–51.

36 Chong P-P, Selvaratnam L, Abbas AA et al. Human peripheral blood derived mesenchymal stem cells demonstrate similar characteristics and chondrogenic differentiation potential to bone marrow derived mesenchymal stem cells. J Orthop Res 2012;30:634–642.

37 Carreras A, Almendros I, Acerbi I et al. Obstructive apneas induce early release of mesenchymal stem cells into circulating blood. Sleep 2009;32:117–119.

38 Ukai R, Honmou O, Harada K et al. Mesenchymal stem cells derived from peripheral blood protects against ischemia. J Neurotrauma 2007;24:508–520.

39 Rochefort GY, Delorme B, Lopez A et al. Multipotential mesenchymal stem cells are mobilized into peripheral blood by hypoxia. Stem Cells 2006;24:2202–2208.

40 Wang Y, Johnsen HE, Mortensen S et al. Changes in circulating mesenchymal stem cells, stem cell homing factor, and vascular growth factors in patients with acute ST elevation myocardial infarction treated with primary percutaneous coronary intervention. Heart 2006;92:768–774.

41 Wu GD, Nolta JA, Jin Y-S et al. Migration of mesenchymal stem cells to heart allografts during chronic rejection. Transplantation 2003;75:679–685.

42 Zvaifler NJ, Marinova-Mutafchieva L, Adams G et al. Mesenchymal precursor cells in the blood of normal individuals. Arthritis Res 2000;2:477–488.

43 Mansilla E, Marín GH, Drago H et al. Bloodstream cells phenotypically identical to human mesenchymal bone marrow stem cells circulate in large amounts under the influence of acute large skin damage: New evidence for their use in regenerative medicine. Transplant Proc 2006;38:967–969.

44 Trivanović D, Kocić J, Mojsilović S et al. Mesenchymal stem cells isolated from peripheral blood and umbilical cord Wharton's jelly. Srp Arh Celok Lek 2013;141:178–186.

45 Kassis I, Zangi L, Rivkin R et al. Isolation of mesenchymal stem cells from G-CSF-mobilized human peripheral blood using fibrin microbeads. Bone Marrow Transplant 2006;37:967–976.

46 Wexler SA, Donaldson C, Denning-Kendall P et al. Adult bone marrow is a rich source of human mesenchymal "stem" cells but umbilical cord and mobilized adult blood are not. Br J Haematol 2003;121:368–374.

47 Lazarus HM, Haynesworth SE, Gerson SL et al. Human bone marrow-derived mesenchymal (stromal) progenitor cells (MPCs) cannot be recovered from peripheral blood progenitor cell collections. J Hematother 1997;6:447–455.

48 Guihard P, Danger Y, Brounais B et al. Induction of osteogenesis in mesenchymal stem cells by activated monocytes/macrophages depends on oncostatin M signaling. Stem Cells 2012;30:762–772.

49 Nicolaidou V, Wong MM, Redpath AN et al. Monocytes induce STAT3 activation in human mesenchymal stem cells to promote osteoblast formation. PLoS One 2012;7:e39871.

50 Scotti C, Piccinini E, Takizawa H et al. Engineering of a functional bone organ through endochondral ossification. Proc Natl Acad Sci USA 2013;110:3997–4002.

See www.StemCellsTM.com for supporting information available online.

Peripheral Blood-Derived Mesenchymal Stem Cells: Candidate Cells Responsible for Healing Critical-Sized Calvarial Bone Defects

Shaowei Li, Ke-Jung Huang, Jen-Chieh Wu, Michael S. Hu, Mrinmoy Sanyal, Min Hu, Michael T. Longaker and H. Peter Lorenz

The online version of this article, along with updated information and services, is located on the World Wide Web at:
http://stemcellstm.alphamedpress.org/content/early/2015/03/04/sctm.2014-0150
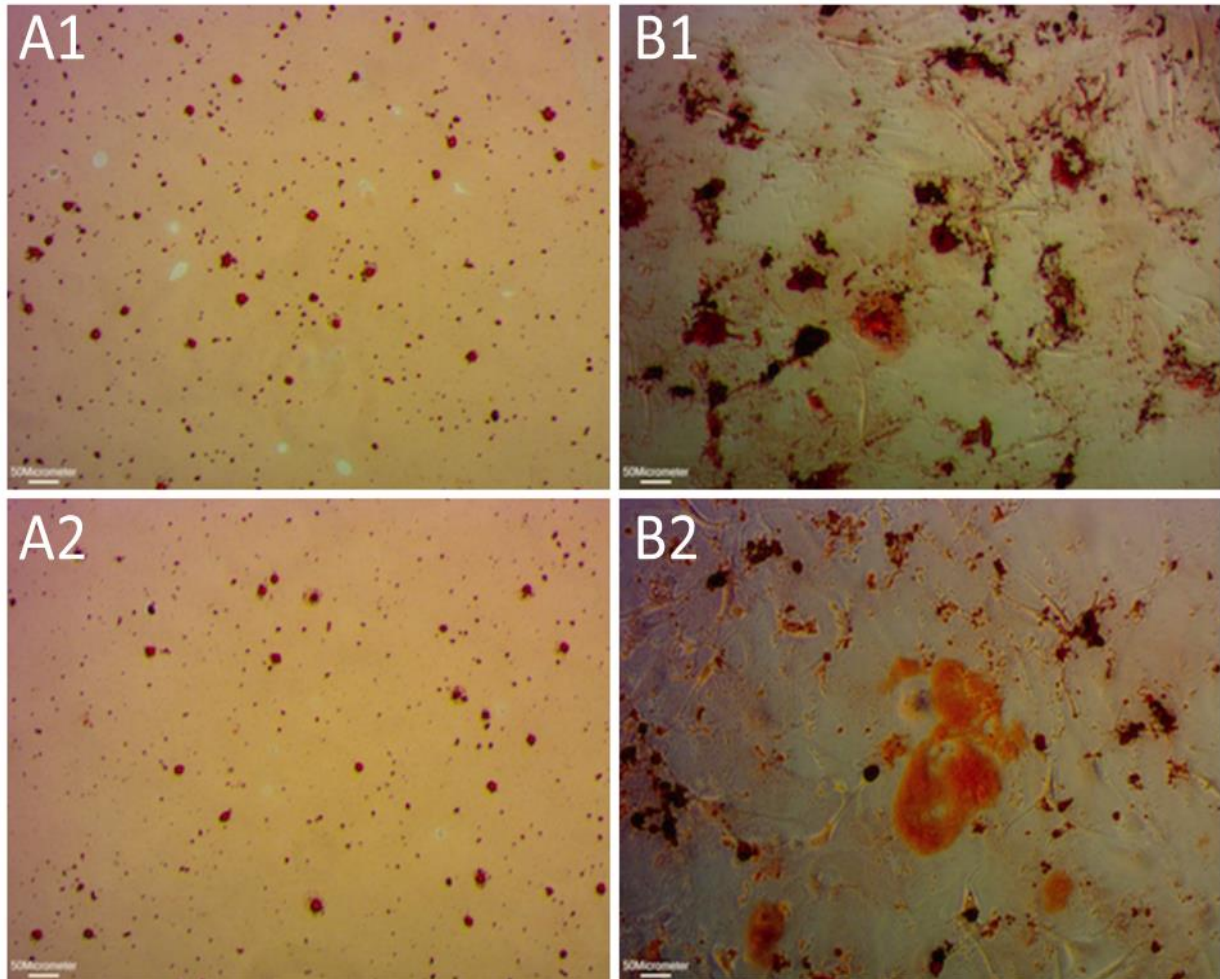
Figure S1. CD45^{+} cells exhibit minor calcification activity in an *in vitro* osteogenic assay. A homogeneous population of CD45^{+} cells (passage 0) from pop2 were seeded to tissue culture dishes and subjected to *in vitro* osteogenic induction followed by staining of calcification deposition by Alizarin Red S. As a positive control for the assay, a population of 20% CD45^{-}/80% CD45^{+} cells (passage 0) from pop1, determined by FACS, were also subjected to the same assay. The homogeneous population of CD45^{+} cells (A1, A2) only displayed minor Alizarin Red S staining indicative of very weak osteogenic activity. The population of 20% CD45^{-}/80% CD45^{+} cells (B1, B2) displayed much stronger Alizarin Red S staining indicative of osteogenic activity contributed by CD45^{-} cells. The scale bar on each panel represents 50 micrometers.
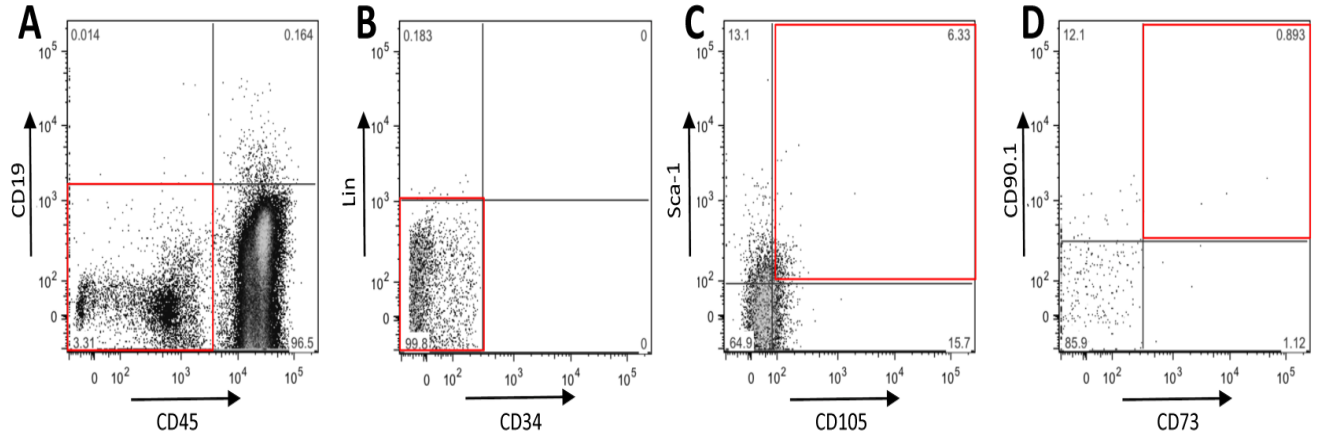
Figure S2. Investigation of freshly isolated peripheral blood for the existence of cells with BD-MSC surface markers. Nucleated cells from peripheral blood were stained with a mixture of fluorophore-conjugated monoclonal antibodies (anti-CD45/APC, anti-CD19/ Alexa Flour®700, anti-Lineage/Pacific Blue, anti-CD34/ PE/Cy5, anti-CD105/ Alexa Flour®488, anti-Sca-1/APC-Cy7, anti-CD73/PE, and anti-CD90.1/PerCp-cy5.5) and subjected to flow cytometry analysis. The CD45$^-$/CD19$^-$ population (red rectangle in panel A) was gated to analyze expression of CD34 and Lin. The resulting CD34$^-$/Lin$^-$ population (red rectangle in panel B) was gated to analyze expression of CD105 and Sca-1. The resulting CD105$^+$/Sca-1$^+$ population (red rectangle in panel C) was gated to analyze expression of CD73 and CD90.1. The final CD73$^+$/CD90.1$^+$ population (red rectangle in panel D) represents the population of CD45$^-$/CD19$^-$/CD34$^-$/Lin$^-$/CD105$^+$/Sca-1$^+$/ CD73$^+$/CD90.1+, which represent approximately 0.0019% (3.31% x 99.8% x 6.33% x 0.89%) of nucleated peripheral blood cells.
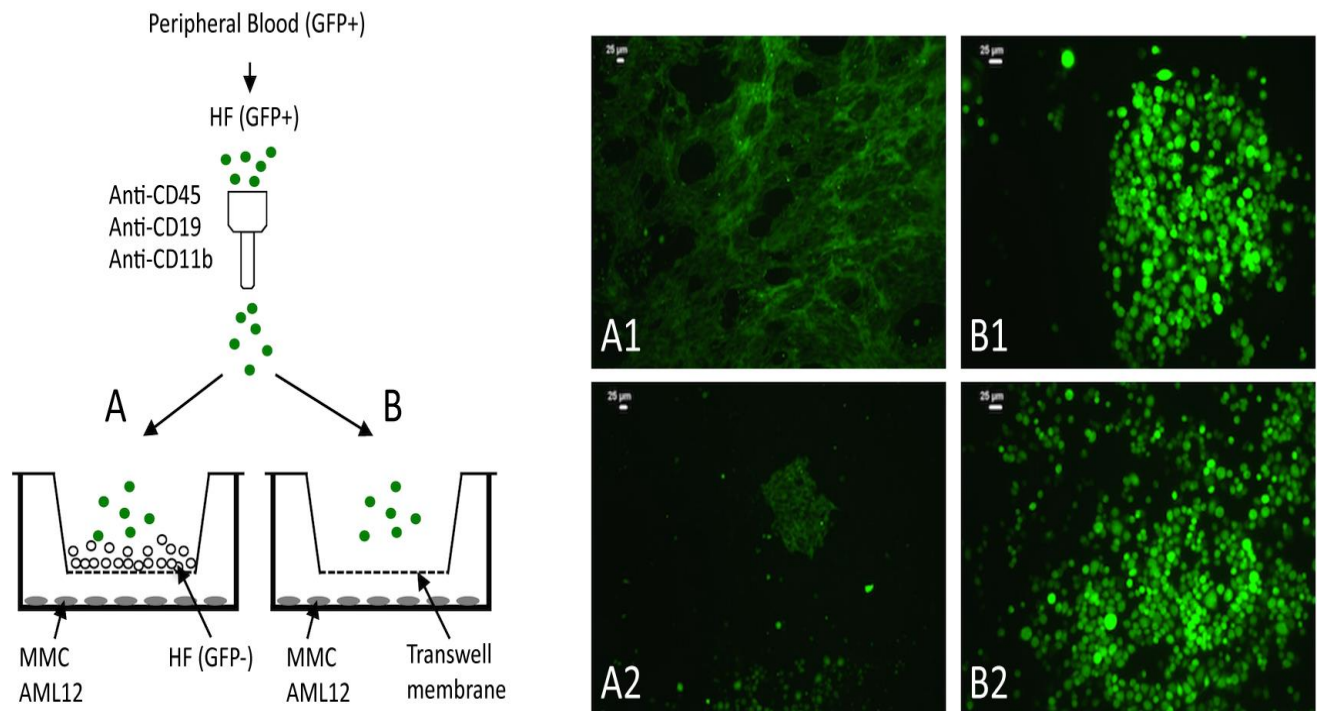
Figure S3. Cultivation of BD-MSCs requires heavy fraction cells. Diagram on the left: Heavy fraction cells (green round dots) from GFP$^+$ FVB-L2G mice were isolated (see Figure 1A) and subjected to MACS MicroBead sorting, in which, anti-CD45, anti-CD19, and anti-CD11b were used to deplete cells expressing corresponding surface markers. The resultant flow-through represented an enriched population of CD45$^-$/ CD19$^-$/CD11b$^-$ cells, which possibly contains the circulating cells of origin of the BD-MSC population. The flow-through was seeded on transwell inserts in the presence (A) or absence (B) of GFP$^-$ HF cells (empty circles) in our AML12 co-culture system. GFP$^-$ HF cells were prepared from FVB mice. Panels on the right: GFP$^+$ BD-MSCs appeared only on the transwell inserts that also contained GFP$^-$ HF cells (A1 and A2). The scale bar on each panel represents 25 micrometers. GFP$^+$ cells that appeared in the absence of HF (B1 and B2) were round shaped and did not have the fibroblastic BD-MSC phenotype. The scale bar on each panel represents 25 micrometers. Thus, BD-MSC production is dependent on the presence of other cells within the heavy fraction (see Figure 1A).